Jet clustering dependence of VBF Higgs production

Michael Rauch and Dieter Zeppenfeld

Institute for Theoretical Physics, Karlsruhe Institute of Technology (KIT), Germany

Precise predictions for Higgs production via vector-boson fusion play an important role when testing the properties of the Higgs boson and probing new-physics effects. While the inclusive cross section changes little when including NNLO and N3LO QCD corrections, a differential NNLO calculation with typical VBF cuts [1] shows large corrections of up to 10% in distributions.

In this article, we investigate the dependence of the differential NNLO QCD calculation on the jet definition. Starting from the known results at a fixed jet clustering choice, we use the electroweak $H+3$ jets production cross section at NLO precision to derive NNLO results for $H+2$ jets production for other jet definitions. We find that larger clustering radii significantly reduce the impact of NNLO corrections. The sizable NNLO corrections for distributions are largely caused by the broader energy flow inside jets at NNLO and are to be expected generally for processes with jets at LO.

I. INTRODUCTION

With the discovery of the Higgs boson [2, 3] at the Large Hadron Collider (LHC) at CERN in 2012, all particles predicted by the Standard Model (SM) have finally been observed. One of the remaining tasks is to verify that it is indeed the SM Higgs which has been observed. For this, a detailed study of its properties, in particular its couplings, needs to be carried out with high precision.

The vector-boson-fusion (VBF) production mode of the Higgs boson is a crucial ingredient for this task [4–14]. Its cross section is sizable, being the second largest one for Higgs production, after gluon fusion. The process exhibits a characteristic feature, two energetic jets in the forward and backward regions of the detector, the so-called tagging jets [15]. The decay products of the Higgs boson are typically more central and in-between them. Also, the Higgs boson is typically produced with considerable transverse momentum. These can be exploited in the kinematic reconstruction of the decay products, e.g. in decays into τ pairs [16–18], or for invisible decay modes [19–21]. Additionally, the nature of the HVV vertex can be probed through the azimuthal-angle distribution of the tagging jets [22, 23].

In order to make full use of the LHC data, precise knowledge and good understanding of the SM prediction of VBF-H production is crucial. The next-to-leading order (NLO) QCD corrections [24–26] have been known for quite some time and yield corrections of $\mathcal{O}(10\%)$. Choosing the momentum transfer of the exchanged virtual bosons as central scale proves to be a good choice to minimize the QCD corrections. The NLO EW corrections are of a similar size [27–29], with opposite sign for inclusive cross sections. Inclusive cross sections have been calculated to next-to-next-to-leading order (NNLO) QCD in Refs. [30, 31] and to next-to-next-to-next-to-leading order (N3LO) in Ref. [32], using the structure-function approach in both cases. The effects are around the percent level for NNLO and at a few per mille for N3LO. The latter further reduces the associated scale uncertainty.

NNLO effects on differential distributions have been studied in the VBF approxima-

tion [1], where QCD corrections to the two quark lines are considered as independent, analogous to the structure-function approach. The effects turn out to be sizable, yielding a reduction of around 6% for the fiducial cross section with typical VBF cuts (high invariant mass and large rapidity separation of the tagging jet pair), and even larger corrections are found for distributions which has been surprising, given the smallness of corrections for inclusive cross sections.

One should bear in mind, however, that the VBF cross sections at LO are completely independent of the jet definition scheme, due to the large rapidity separation enforced by the VBF cuts. Even in an NLO cross section, the internal jet shape is only modeled by up to two partons, i.e. any dependence on the jet algorithm or the jet radius in the rapidity-azimuthal angle-plane is modeled at LO only. Indeed it was found long time ago that the jet shape of current jets in DIS, which have the same properties as the tagging jets in VBF, is much wider at NLO, when up to three partons model the internal energy flow [33]. These effects will lead to differences in jet algorithm and jet radius dependencies for NNLO as compared to NLO cross sections.

In this paper, we investigate the dependence of the differential NNLO cross section on the definition of the jets. We test how different choices change the size of the corrections, and where features are insensitive to the jet definition.

II. SETUP

As starting point for our investigation we use the results of the differential NNLO QCD calculation presented in Ref. [1], and we follow the setup chosen there. Specifically, we study VBF-H production

$$pp \to Hjj + X \tag{1}$$

in proton-proton collisions with a center-of-mass energy of $\sqrt{s} = 13$ TeV. As parton distribution function we use the NNPDF 3.0 set at NNLO with $\alpha_S(M_Z) = 0.118$ (NNPDF30_nnlo_as_0118) [34] throughout. Bottom quarks are taken as massless and their effects are included, while top-quark effects are excluded both as final state and in internal lines. The CKM matrix is taken as diagonal. The Higgs boson is produced on-shell, while for the W and Z boson propagators we use full Breit-Wigner propagators. The masses, widths and the Fermi constant are set to

$$
\begin{aligned}
M_W &= 80.398 \text{ GeV}, & \Gamma_W &= 2.141 \text{ GeV}, \\
M_Z &= 91.1876 \text{ GeV}, & \Gamma_Z &= 2.4952 \text{ GeV}, \\
M_H &= 125 \text{ GeV}, & G_F &= 1.16637 \times 10^{-5} \text{ GeV}^{-2}.
\end{aligned}
\tag{2}
$$

The remaining electroweak parameters are calculated from the W and Z masses and G_F via electroweak tree-level relations. As scale we use

$$\mu^2 = \frac{M_H}{2} \sqrt{\left(\frac{M_H}{2}\right)^2 + p_{T,H}^2}. \tag{3}$$

By default, jets are clustered from partons using the anti-k_T algorithm [35] with separation parameter $R = 0.4$. Each event must contain at least two jets with

$$p_{T,j} > 25 \text{ GeV}. \tag{4}$$

To pass the VBF cuts, the two tagging jets, defined as the two jets of highest p_T, must fulfill

$$|y_j| < 4.5 \qquad\qquad y_{j1} \times y_{j2} < 0$$
$$m_{j1,j2} > 600 \text{ GeV} \qquad\qquad \Delta y_{j1,j2} > 4.5 \qquad\qquad , \qquad (5)$$

i.e. they must be located in opposite hemispheres, well-separated in rapidity, and the pair must have a large invariant mass.

To study the impact of the jet clustering, let us first consider the effect of the algorithm. We restrict ourselves here to the family of sequential recombination jet algorithms [35], with the variants anti-k_T, Cambridge/Aachen (C/A), and k_T, which correspond to the exponent parameter $n = -1, 0$, and 1, respectively. Since the algorithm is a function of the momenta of the final-state partons, loop effects have a strongly diminished influence as compared to real emission corrections. For two-parton final states, both partons need to be identified as jets for the event to pass the selection cuts, Eqs. (4,5). Therefore, from the rapidity separation cut it follows that the separation of the two partons is at least as large, $R_{jj} > 4.5$. This is well above any reasonable values for the R parameter of the jet algorithm, so for two-parton kinematics the choice of R has no effect. As a result, the two-loop contributions to the NNLO cross section do not influence jet-algorithm- or R-dependence. Three-parton final states exhibit a dependence on R, which determines whether the third parton is clustered with either of the leading partons. However, there is as yet no dependence on the exponent, n, since, with at most one parton pair available for a jet, the p_T-ordering of partons has no consequence. Algorithm dependence only enters with four-parton events. When both additional partons are inside the cone of one of the leading partons, the order of recombination can become relevant and give different results. We note that this dependence on the parameters R and n is shifted by one compared to the general case of $X + 1$ jet cross sections, where already for three-parton events both parameters are relevant. This is a consequence of the rapidity-separation cut in VBF processes, which enforces a very large R separation between at least two partons.

Analogous to the study of jet shapes in NNLO DIS cross sections in Ref. [33], which was performed with an NLO $ep \rightarrow jj + X$ code, to study jet definition effects in NNLO VBF cross sections, it is sufficient to use a sample of VBF $H+3$ jets events at NLO QCD [36, 37]. These include the necessary interference of tree level and 1-loop contributions for 3-parton final states and the 4-parton double-real parts of the VBF-H NNLO QCD calculation. We generate these events with process ID 110 in VBFNLO [38–40], using the parameter settings given in Eqs. (2,3) and the cuts of Eqs. (4,5).

Our starting point, the NNLO QCD calculation of Ref. [1], already contains these contributions for a specific value of R and n, namely $R = 0.4$ and $n = -1$ (anti-k_T). Therefore, to go to different values we can use the $H+3$ and $H+4$ parton integrals which contribute to the calculation of the NLO $Hjjj$ cross section to define correction terms $\Delta(R, n)$ such that

$$\mathrm{d}\sigma_{Hjj}^{\mathrm{NNLO}}(R, n) = \mathrm{d}\sigma_{Hjj}^{\mathrm{NNLO}}(R{=}0.4, n{=}{-}1) \underbrace{-\mathrm{d}\sigma_{H3+}^{\mathrm{NLO}}(R{=}0.4, n{=}{-}1) + \mathrm{d}\sigma_{H3+}^{\mathrm{NLO}}(R, n)}_{=\Delta(R,n)} . \qquad (6)$$

We subtract the contribution for the base values from the differential cross section and add back the same terms for the desired new values. The $\mathrm{d}\sigma_{H3+}^{\mathrm{NLO}}$ denote the sum of 3-parton and 4-parton contributions which, when clustered with 3-jet cuts, would give the NLO $Hjjj$ cross section. However now, after clustering with parameters (R, n), only 2 hard jets

are required by the cut function.[1] The full NNLO differential cross section would contain additional 2-parton contributions (two-loop virtual terms, subtraction terms for double soft or collinear 4-parton configurations, subtraction terms for virtual soft or collinear terms, finite collinear pieces etc.), however any 2-parton contributions are independent of (R, n) and therefore exactly cancel in the difference $\Delta(R, n)$. For 3- and 4-parton configurations the two terms of $\Delta(R, n)$ will in general have a different kinematic structure for the jets. So the VBF cuts apply individually to each of the two terms in $\Delta(R, n)$. Similarly, when histogramming the events, the terms might go into different bins of the distribution.

To better understand why the subtraction terms of the NLO $Hjjj$ cross section are also sufficient for the calculation of $\Delta(R, n)$, let us consider the phase space regions of non-vanishing $\Delta(R, n)$. For each 3- or 4-parton configuration passing the VBF cuts we can identify the two leading (highest p_T) hard partons, which are at the center of the two tagging jets, by running the clustering algorithm. A non-vanishing $\Delta(R, n)$ requires at least one hard additional parton with separation from one of the leading partons (or pre-cluster of partons) in the interval $(0.4, R)$. If the clusters for $(R = 0.4, n = -1)$ and (R, n) differ only by sufficiently soft partons (or not at all), both jet parameter choices will yield practically the same jets which end up in identical histogram bins, i.e. one gets $\Delta(R, n) = 0$. A well separated hard additional parton gives a finite contribution to the integral of 3-parton configurations, and in a 4-parton configuration the usual subtraction term for a soft or collinear fourth parton will render the integral over this last parton finite.

Technically, we first generate weighted events with no restrictions on the phase-space of the partons, both for three-parton kinematics, comprising the Born and virtual contributions of the VBF $H+3$ jets cross section, and for four-parton kinematics for the real-emission part. Then for all required (R, n) combinations the jet clustering algorithm is applied to the event. If it passes the jet cuts of Eqs. (4,5), the weight of the event is booked in the corresponding histogram bin, taking into account the minus sign for the middle term in Eq. (6). To steer the Monte-Carlo integration, we finally check if any (R, n) combination has passed all cuts. If not, the event weight is set to zero. Otherwise, in order to improve Monte Carlo convergence, we weight the event with the largest differences of m_{jj} and Δy_{jj} between all considered (R, n) and the reference value of $(R=0.4, n=-1)$. For example, in a 2-jet configuration where three of the partons are very collinear and are always clustered into the same jet, the weight factor would become exactly zero, corresponding to the fact that in that case also $\Delta(R, n)$ vanishes. Similarly, if one of the partons becomes soft, its effect on m_{jj} and Δy_{jj} becomes small, so that in the infrared limit the weight factor also approaches zero. Note that this factor is only used to steer the integration and does not enter the physical weights used for the histograms.

An identity similar to Eq. (6) relates the NLO result for arbitrary values of R with the NLO result for $R = 0.4$ and the LO matrix elements for VBF $H+3$ jets production, $\mathrm{d}\sigma_{Hjj}^{\mathrm{NLO}}(R) = \mathrm{d}\sigma_{Hjj}^{\mathrm{NLO}}(R=0.4) - \mathrm{d}\sigma_{H3}^{\mathrm{LO}}(R=0.4) + \mathrm{d}\sigma_{H3}^{\mathrm{LO}}(R)$. We have checked that the differential cross section obtained in this way agrees with a calculation where the jet clustering radius has been explicitly set to R. The level of agreement is better than one per mill. To verify our setup, we have also cross-checked our results for the integrated and differential LO and NLO cross sections generated by VBFNLO with the results from Ref. [1] and find that they are consistent within the statistical errors from Monte-Carlo integration.

---

[1] Here the cut function is defined as the step-function, multiplying the squared matrix elements, which specifies whether a phase space configuration satisfies all cuts and belongs to a specific histogram bin.

III.   RESULTS

In Fig. 1 we first show the integrated cross section as a function of the jet clustering radius R. At LO, where only two partons are available, the cross section is independent of the value of R, as discussed above. The NLO cross section then exhibits a dependence on R, leading to an 8.5% reduction at the reference value $R = 0.4$. Going to larger values, the NLO cross section rises, at about $R = 1.0$ it coincides with the LO value, and surpasses it when R becomes even larger. Going one order higher in the perturbative expansion, the NNLO cross section exhibits an even stronger R dependence. At the reference value, $R = 0.4$, a further 6% reduction of the cross section compared to NLO takes place. Again around $R = 1.0$, the NNLO cross section agrees with both the LO and NLO results. Therefore, we choose $R = 1.0$ as a matching point in the following, when studying differential distributions. For all three curves, we also show the effect of varying the scale by a factor between 0.5 and 2 around the central scale given in Eq. (3), indicated by the underlying band. The sizable scale dependence of the LO results is significantly reduced when going to NLO, while going one order further to NNLO yields only a small additional reduction. For all combinations, the scale variation bands are not overlapping at the reference value. We also note that for NLO, the position of the plateau coincides well with the central scale choice when taking the matching point, $R = 1.0$.

Looking at distributions, we first consider the transverse momentum of the leading jet, shown in Fig. 2. The left panel shows the results for $R = 0.4$, where the NNLO curve has been taken from Ref. [1]. The center panel uses the matching point with an R value of 1.0, and in the right panel we present results with $R = 1.6$ for comparison. Using the reference value $R = 0.4$, we see a reduction of the differential cross section over most of the shown range, which is approximately a constant factor for transverse momenta larger than 100 GeV.
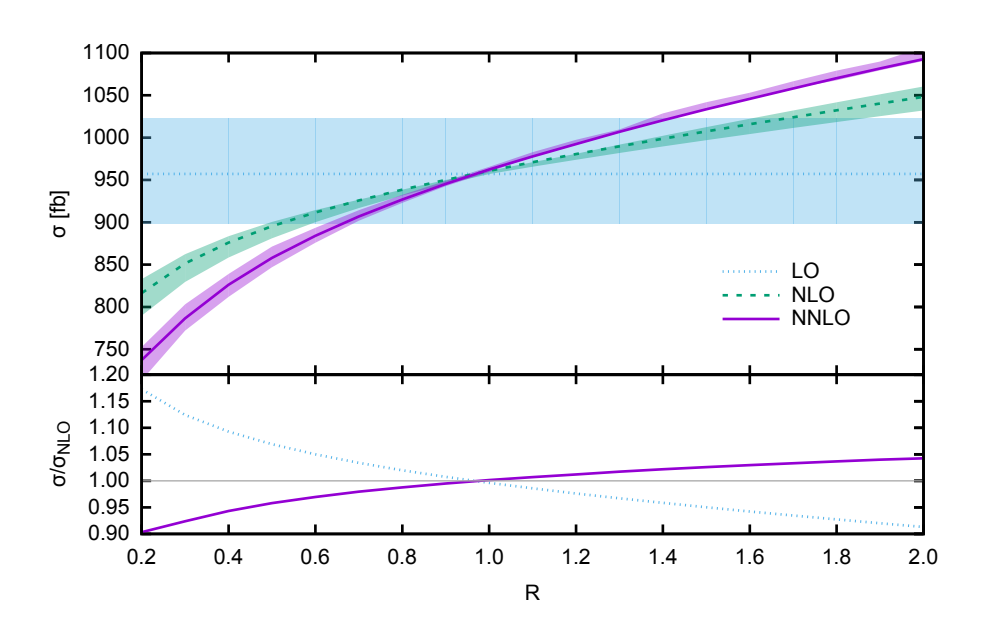

FIG. 1. Integrated cross section for VBF-H production as function of the jet clustering radius R using the setup and cuts of Eqs. (2,3,4,5). The respective bands arise from a scale variation by a factor $[0.5; 2]$ around the central scale μ. The numerical value of the NNLO cross section at $R = 0.4$ is taken from Ref. [1].
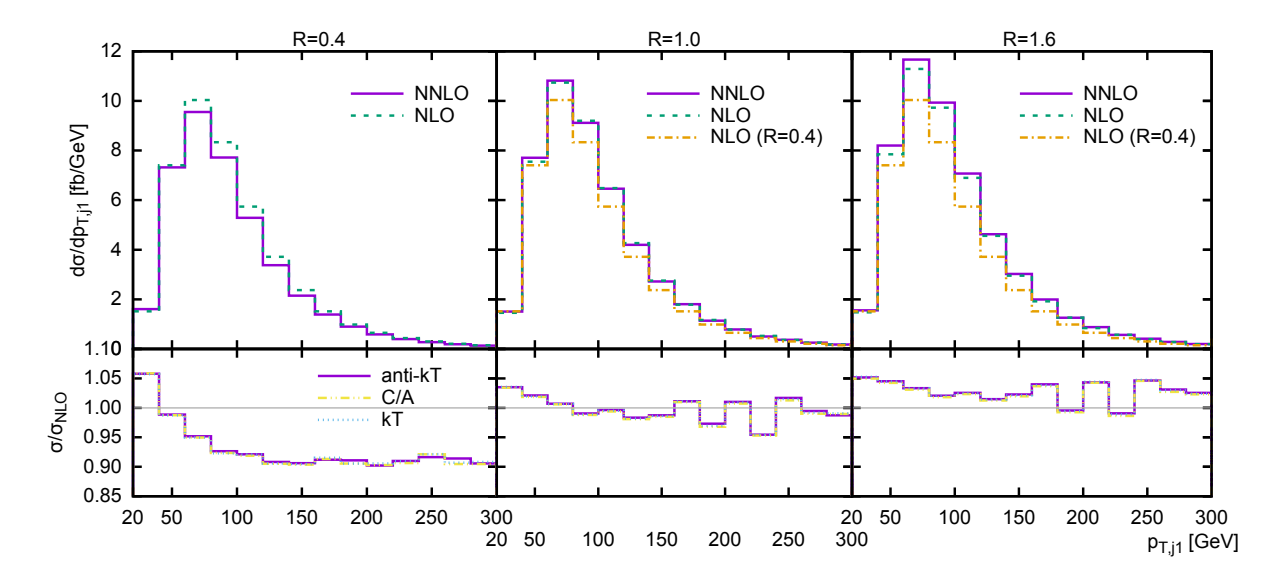
FIG. 2. Transverse momentum distribution of the leading jet. Results are shown for R values of 0.4 (*left*), 1.0 (*center*) and 1.6 (*right*).

For smaller transverse momenta, the corrections decrease and in the first bin the additional NNLO effects give a positive contribution to the cross section. Employing our matching value, $R = 1.0$, we see that for jet transverse momenta above 80 GeV, the NLO and NNLO results roughly agree within the statistical errors. For comparison, we have again plotted the $R=0.4$ NLO curve in the upper panel. It shows that both the NLO and NNLO curves have shifted upwards, consistent with the behavior seen for the integrated cross section in Fig. 1. Only in the first two bins there is still a significant positive correction, but with a smaller relative size than for $R = 0.4$. In the right panel with $R = 1.6$, we finally see that the NNLO contributions are always positive. In the lower ratio panels, we additionally show the effect from using the Cambridge/Aachen and k_T clustering algorithm instead of our default choice of anti-k_T. The effects due to different cluster algorithms are tiny. We have checked that this also holds for all other distributions. Therefore, we will show further distributions only for the anti-k_T algorithm.

In Fig. 3, we show the distribution of the rapidity difference of the two tagging jets, again for the three jet clustering radii of $R = 0.4$, 1.0 and 1.6. For the reference value, the ratio of NNLO over NLO cross sections is below one for values close to the lower cut at $\Delta y_{j1,j2} = 4.5$. They then become gradually larger until a large positive correction is reached at the upper limit of 9, which is given by the requirement that the absolute value of the jet rapidity is below 4.5. Moving to the larger $R = 1.0$ clustering, the additional NNLO corrections become small up to a rapidity difference of about 7. Only for larger values do we see significant remaining contributions, which are positive in size. Thereby, the phase-space region of large rapidity difference and small transverse momenta of the leading jet is connected. As the cut on the invariant mass of the two tagging jets requires the jets to be very energetic, a small transverse momentum causes a large rapidity of each jet, and thus a large rapidity difference. The distribution for $R = 1.6$ exhibits a behavior similar to the one for $R = 1.0$, namely a constant correction factor for lower rapidity differences with a rise towards larger ones. Due to the larger jet radius, the correction factor is larger than one throughout.
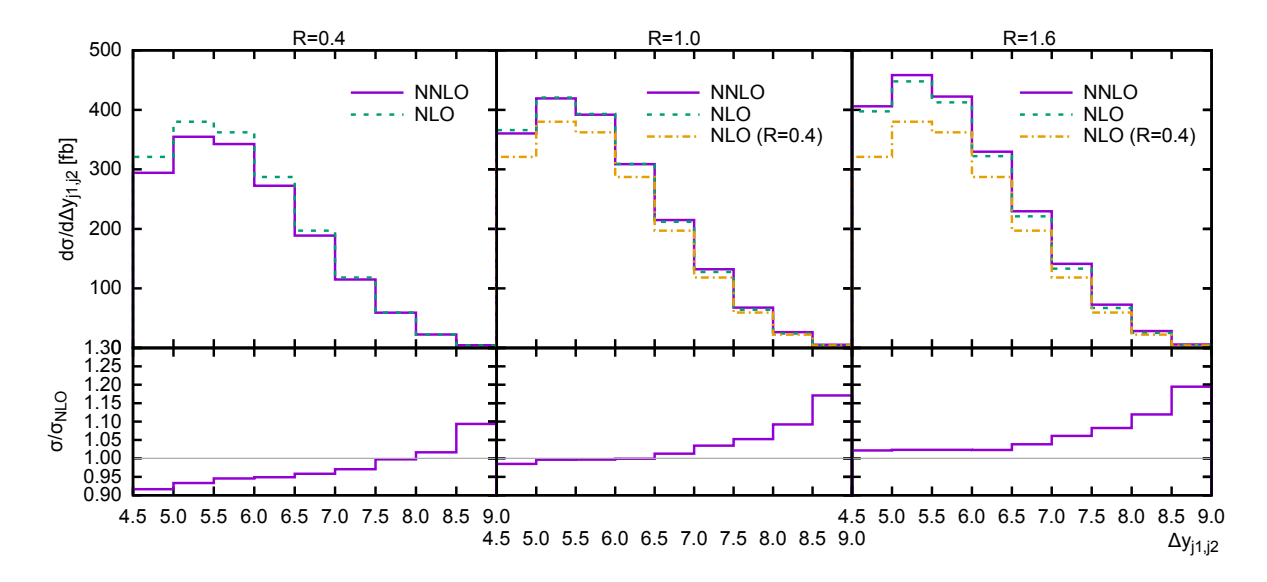
FIG. 3. Rapidity difference of the two tagging jets. Results are shown for R values of 0.4 (*left*), 1.0 (*center*) and 1.6 (*right*).
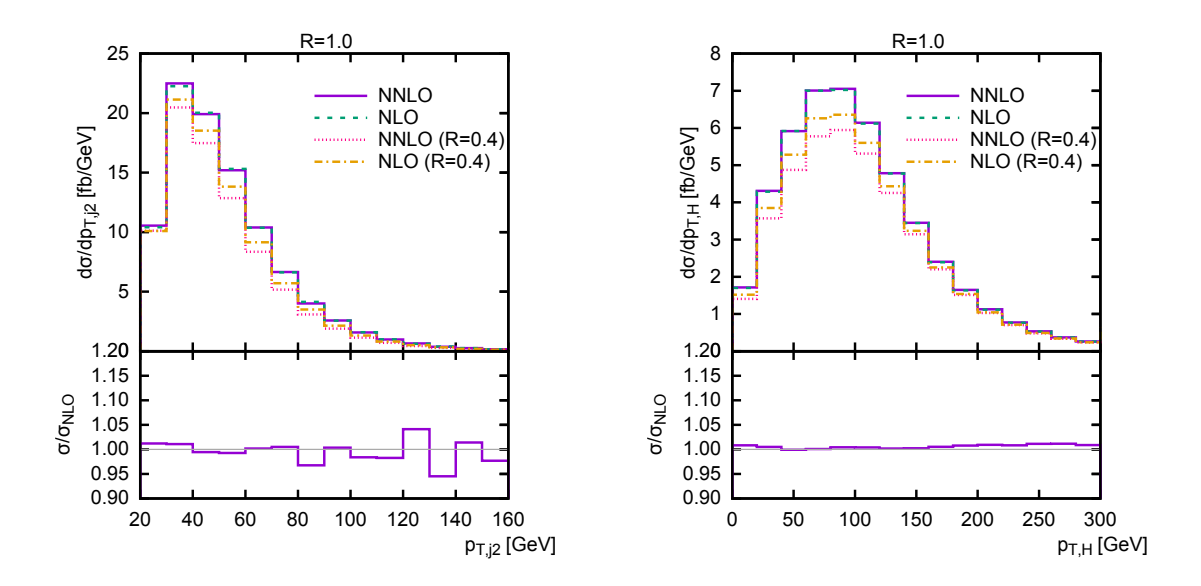

FIG. 4. Transverse momentum distributions of the second jet (*left*) and of the Higgs boson (*right*).

In Fig. 4 we finally show two more distributions, namely the transverse momentum of the second jet on the left and the transverse momentum of the Higgs boson on the right, showing only results for the matching value of $R = 1.0$. In both cases, the larger jet clustering radius reduces the size of the NNLO corrections to very small values over the whole range of the distribution. In contrast, at $R = 0.4$ the ratio of NNLO over NLO results for these two distributions ranges between 0.9 and 1.0 [1] and thus shows sizable NNLO corrections. Obviously, these large corrections are due to the wider energy flow inside the tagging jets, which is captured to a larger degree by the $R = 1.0$ jets than by the narrow $R = 0.4$ jets used in many LHC analyses.

IV. DISCUSSION AND CONCLUSIONS

The NNLO cross section for VBF-Hjj production shows a remarkably strong dependence on the jet definition, in particular on the jet radius in the rapidity-azimuthal angle-plane. Starting with the results of the NNLO calculation for a given jet algorithm, we use the NLO QCD calculation of VBF $H+3$ jets production to calculate the NNLO cross section at different values of both the jet clustering radius R and the momentum exponent, corresponding to the choices of anti-k_T, Cambridge/Aachen and k_T.

We find that a large jet clustering radius of $R = 1.0$ leads to small NNLO corrections to the fiducial VBF cross section (within the VBF cuts of Eqs.(5)). This also holds for most differential distributions. Relevant NNLO corrections remain in a phase-space region where the transverse momenta of both jets are small, and therefore the rapidity separation between them becomes large. Effects from choosing different jet clustering exponents are tiny.

The strong R-dependence of differential distributions and fiducial cross sections can be explained by the wider energy flow within quark jets at NNLO QCD, which was first discussed quantitatively for DIS jets in ep-scattering [33]: a larger jet radius captures a larger fraction of the energy of the original scattered quark and thus leads to an increase in average jet energy. Tagging jets defined with larger R thus have larger dijet invariant mass and they more easily pass the $m_{jj} > 600$ GeV cut of the VBF selection. The resulting increase in fiducial cross section, exhibited in Fig. 1, is substantial, reaching 17 percent when comparing $R = 0.4$ and $R = 1.0$, with a 6 percent shift due to NNLO effects alone, a surprisingly large contribution when compared to the considerably smaller NNLO corrections to the inclusive VBF Hjj cross section. These sizable corrections become intuitively understandable, however, when remembering that any R-dependence is determined at one order lower in perturbation theory than the cross section itself, i.e. in the NNLO cross section, R-dependence is modeled with NLO accuracy only.

The observed large corrections to jet shape and R-dependence, in going from NLO to NNLO modeling, are not captured by a scale variation of NLO cross sections. They should be treated as an additional uncertainty in any NLO cross section calculation for processes which exhibit jets at LO already. From our example of VBF Higgs production, one should assign an additional, order 10% uncertainty to NLO cross sections with quark jets in the final state, which becomes especially relevant when the scale variation of the NLO cross section is exceptionally small, like in VBF. For processes with gluon jets at LO, these corrections are expected to be larger, because of the enhanced radiation from gluons due to their larger color charge. Also, cross sections with steeper jet transverse momentum dependence at LO should be affected more by energy flow corrections in NNLO calculations than the VBF distributions, which have relatively mild p_T-dependence of the tagging jets.

We found very small NNLO corrections for fiducial VBF cross sections and distributions for tagging jets defined with a radius $R = 1.0$. This does not mean, of course, that analyses at the LHC for VBF processes should be performed with such fat jets, since contributions from underlying event or pile-up would lead to additional large corrections, which may well induce higher cross section uncertainties than N3LO effects, which are still missing in the discussion above. Such investigations go beyond the aim and scope of the present paper, however.

ACKNOWLEDGMENTS

---

[1] M. Cacciari, F. A. Dreyer, A. Karlberg, G. P. Salam, and G. Zanderighi, Phys. Rev. Lett. **115**, 082002 (2015), arXiv:1506.02660 [hep-ph].

[2] G. Aad *et al.* (ATLAS), Phys. Lett. **B716**, 1 (2012), arXiv:1207.7214 [hep-ex].

[3] S. Chatrchyan *et al.* (CMS), Phys. Lett. **B716**, 30 (2012), arXiv:1207.7235 [hep-ex].

[4] R. N. Cahn and S. Dawson, Phys. Lett. **B136**, 196 (1984), [Erratum: Phys. Lett.B138,464(1984)].

[5] S. Dawson, Nucl. Phys. **B249**, 42 (1985).

[6] M. J. Duncan, G. L. Kane, and W. W. Repko, Nucl. Phys. **B272**, 517 (1986).

[7] R. N. Cahn, S. D. Ellis, R. Kleiss, and W. J. Stirling, Phys. Rev. **D35**, 1626 (1987).

[8] R. Kleiss and W. J. Stirling, Phys. Lett. **B200**, 193 (1988).

[9] V. D. Barger, T. Han, and R. J. N. Phillips, Phys. Rev. **D37**, 2005 (1988).

[10] J. M. Butterworth, B. E. Cox, and J. R. Forshaw, Phys. Rev. **D65**, 096014 (2002), arXiv:hep-ph/0201098 [hep-ph].

[11] S. Dittmaier *et al.* (LHC Higgs Cross Section Working Group), (2011), 10.5170/CERN-2011-002, arXiv:1101.0593 [hep-ph].

[12] S. Dittmaier *et al.*, (2012), 10.5170/CERN-2012-002, arXiv:1201.3084 [hep-ph].

[13] J. R. Andersen *et al.* (LHC Higgs Cross Section Working Group), (2013), 10.5170/CERN-2013-004, arXiv:1307.1347 [hep-ph].

[14] M. Rauch, (2016), arXiv:1610.08420 [hep-ph].

[15] D. Zeppenfeld, in *Neutrinos in physics and astrophysics from 10**(-33) to 10**28 CM. Proceedings, Conference, TASI'98, Boulder, USA, June 1-26, 1998* (1999) pp. 303–350, arXiv:hep-ph/9902307 [hep-ph].

[16] T. Plehn, D. L. Rainwater, and D. Zeppenfeld, Phys. Rev. **D61**, 093005 (2000), arXiv:hep-ph/9911385 [hep-ph].

[17] G. Aad *et al.* (ATLAS), JHEP **04**, 117 (2015), arXiv:1501.04943 [hep-ex].

[18] S. Chatrchyan *et al.* (CMS), JHEP **05**, 104 (2014), arXiv:1401.5041 [hep-ex].

[19] O. J. P. Eboli and D. Zeppenfeld, Phys. Lett. **B495**, 147 (2000), arXiv:hep-ph/0009158 [hep-ph].

[20] G. Aad *et al.* (ATLAS), JHEP **01**, 172 (2016), arXiv:1508.07869 [hep-ex].

[21] V. Khachatryan *et al.* (CMS), JHEP **02**, 135 (2017), arXiv:1610.09218 [hep-ex].

[22] T. Plehn, D. L. Rainwater, and D. Zeppenfeld, Phys. Rev. Lett. **88**, 051801 (2002), arXiv:hep-ph/0105325 [hep-ph].

[23] J. R. Andersen, K. Arnold, and D. Zeppenfeld, JHEP **06**, 091 (2010), arXiv:1001.3822 [hep-ph].

[24] T. Han, G. Valencia, and S. Willenbrock, Phys. Rev. Lett. **69**, 3274 (1992), arXiv:hep-ph/9206246 [hep-ph].

[25] T. Figy, C. Oleari, and D. Zeppenfeld, Phys. Rev. **D68**, 073005 (2003), arXiv:hep-ph/0306109 [hep-ph].

[26] E. L. Berger and J. M. Campbell, Phys. Rev. **D70**, 073011 (2004), arXiv:hep-ph/0403194 [hep-ph].

[27] M. Ciccolini, A. Denner, and S. Dittmaier, Phys. Rev. Lett. **99**, 161803 (2007), arXiv:0707.0381 [hep-ph].

[28] M. Ciccolini, A. Denner, and S. Dittmaier, Phys. Rev. **D77**, 013002 (2008), arXiv:0710.4749 [hep-ph].

[29] T. Figy, S. Palmer, and G. Weiglein, JHEP **02**, 105 (2012), arXiv:1012.4789 [hep-ph].

[30] P. Bolzoni, F. Maltoni, S.-O. Moch, and M. Zaro, Phys. Rev. Lett. **105**, 011801 (2010), arXiv:1003.4451 [hep-ph].

[31] P. Bolzoni, F. Maltoni, S.-O. Moch, and M. Zaro, Phys. Rev. **D85**, 035002 (2012), arXiv:1109.3717 [hep-ph].

[32] F. A. Dreyer and A. Karlberg, Phys. Rev. Lett. **117**, 072001 (2016), arXiv:1606.00840 [hep-ph].

[33] N. Kauer, L. Reina, J. Repond, and D. Zeppenfeld, Phys. Lett. **B460**, 189 (1999), arXiv:hep-ph/9904500 [hep-ph].

[34] R. D. Ball *et al.* (NNPDF), JHEP **04**, 040 (2015), arXiv:1410.8849 [hep-ph].

[35] M. Cacciari, G. P. Salam, and G. Soyez, JHEP **04**, 063 (2008), arXiv:0802.1189 [hep-ph].

[36] T. Figy, V. Hankele, and D. Zeppenfeld, JHEP **02**, 076 (2008), arXiv:0710.5621 [hep-ph].

[37] F. Campanario, T. M. Figy, S. Plätzer, and M. Sjödahl, Phys. Rev. Lett. **111**, 211802 (2013), arXiv:1308.2932 [hep-ph].

[38] K. Arnold *et al.*, Comput. Phys. Commun. **180**, 1661 (2009), arXiv:0811.4559 [hep-ph].

[39] J. Baglio *et al.*, (2014), arXiv:1404.3940 [hep-ph].

[40] J. Baglio, J. Bellm, G. Bozzi, M. Brieg, F. Campanario, C. Englert, B. Feigl, J. Frank, T. Figy, F. Geyer, C. Hackstein, V. Hankele, B. Jäger, M. Kerner, M. Kubocz, M. Löschner, L. D. Ninh, C. Oleari, S. Palmer, S. Plätzer, M. Rauch, R. Roth, H. Rzehak, F. Schissler, O. Schlimpert, M. Spannowsky, M. Worek, and D. Zeppenfeld, "VBFNLO - a parton level Monte Carlo for processes with electroweak bosons," `https://www.itp.kit.edu/vbfnlo` (2017).